

Threshold behaviour of effective potential for ${}^{6,7}\text{Li}+{}^{58,64}\text{Ni}$ around the Coulomb barrier

Mili Biswas^{*,1}, Subinit Roy¹, M. Sinha^{1,2}, M. K. Pradhan¹, P. Basu¹, H. Majumdar¹, A. Mukherjee¹, U. Datta Pramanik¹, A. Shrivastava³, K. Ramachandran³

* E-mail: mili.biswas@saha.ac.in

¹ Saha Institute of Nuclear Physics, 1/AF Bidhan Nagar, Kolkata-700064, INDIA

² Gurudas College, Narikeldanga, Kolkata-700054, INDIA

³ Nuclear Physics Division, Bhabha Atomic Research Centre, Mumbai-400085, INDIA

In order to probe the effect of the breakup or transfer induced breakup coupling on the energy dependence of the optical potential in the presence of conventional quasielastic couplings, the elastic scattering angular distributions for ${}^{6,7}\text{Li}$ on ${}^{64}\text{Ni}$ have been measured at Tata Institute of Fundamental Research/Bhabha Atomic Research Centre Pelletron Facility, Mumbai, India. The experiments were carried out in the energy range of $12 \text{ MeV} \leq E_{lab} \leq 26 \text{ MeV}$ near the Coulomb barrier ($\sim 14 \text{ MeV}$) of respective systems. A phenomenological optical model analysis was performed for the systems ${}^6\text{Li}+{}^{64}\text{Ni}$ and ${}^7\text{Li}+{}^{58,64}\text{Ni}$, and the behaviours of the surface strengths of the potential components with decreasing energy were extracted. A further analysis of the measured angular distributions, along with the existing data for ${}^{6,7}\text{Li}+{}^{58}\text{Ni}$, was performed with two different model potentials - one with the folded potential normalized with a complex factor (OMP1) and the other with a *hybrid* potential composed of a renormalized folded real and a phenomenological imaginary (OMP2) potential components. All the model potentials predict similar energy dependent behaviour for the interaction potential around the barrier indicating a model independence of the observed behaviour. The observed energy dependences of the strengths of the real and imaginary potentials also corroborate with the dispersion relation prediction for both the ${}^6\text{Li}+{}^{64}\text{Ni}$ and ${}^6\text{Li}+{}^{58}\text{Ni}$ systems. Though the evidence of breakup is distinct in the energy variation of the potential strengths for ${}^6\text{Li}+{}^{58,64}\text{Ni}$ systems, close to the barrier the variation is more in the line of conventional threshold anomaly. Also the threshold behaviour of the interaction potential does not indicate any distinct isotopic dependence for ${}^6\text{Li}+{}^{58,64}\text{Ni}$. On the other hand, though ${}^7\text{Li}+{}^{64}\text{Ni}$ shows normal threshold behaviour, for ${}^7\text{Li}+{}^{58}\text{Ni}$, the potential does not exhibit any significant energy dependence. Unlike ${}^6\text{Li}$, in case of ${}^7\text{Li}$ a distinct isotopic dependence has been observed for ${}^{58}\text{Ni}$ and ${}^{64}\text{Ni}$.

10th Symposium on Nuclei in the Cosmos

July 27 - August 1, 2008

Mackinac Island, Michigan, USA

1. Introduction

It is the energy dependence of the interaction potential that gives an essence of various reaction mechanisms involved in the nucleus- nucleus collision. For incident energies close to the Coulomb barrier of the colliding system, due to the coupling effects, the optical model potential parameters describing the elastic scattering begin to vary rapidly with energy. In nucleus-nucleus collision, this phenomenon of rapid energy variation of the interaction potential is referred to as ‘Threshold Anomaly’. An attractive dynamic polarization potential, arising out of the channel coupling effects, enhances the real potential near the barrier for the systems involving strongly bound nuclei [1]. In this energy domain the behaviours of the real and the imaginary potentials and their connectivity through a dispersion relation could fully be understood in the case of strongly bound systems. However the difficulty lies in the study of loosely bound nuclei. Some additional reaction channels leading to 3-body final states do exist for loosely bound nuclei and these additional couplings modify the potential behaviour by introducing a repulsive dynamical real polarization potential. Another interesting feature for the systems involving weakly bound projectile is the existence of different threshold behaviour of effective potential for different target mass region. For instance, the energy dependence for ${}^6,7\text{Li}+{}^{208}\text{Pb}$ is very different from that observed in the literature for ${}^6,7\text{Li}+{}^{28}\text{Si}$. In this context, we would like to present our investigation of ${}^6,7\text{Li}$ scattering from ${}^{58,64}\text{Ni}$ isotopes. Unlike the heavy targets, the Coulomb induced breakup at near or sub-barrier energies is not so dominant for Ni-isotopes. Also ${}^{58}\text{Ni}$ and ${}^{64}\text{Ni}$ being similarly deformed ($\beta_2 \sim 0.17$), the effect of coupling to the collective target excitations might be similar. But as ${}^7\text{Li}$ is more strongly bound projectile (breakup threshold = 2.45 MeV, 1st excited state energy = 0.47 MeV) than ${}^6\text{Li}$ (breakup threshold = 1.47 MeV), the couplings to the continuum are expected to be different. One more salient feature for these systems is the difference in the Q-values for the single neutron transfer channel leading to 3-body final states. For ${}^6\text{Li}+{}^{58,64}\text{Ni}$ Q-values for 1n stripping channel are : +3.3 MeV and +0.43 MeV respectively whereas for ${}^7\text{Li}+{}^{58,64}\text{Ni}$ the Q-values are : +1.749 MeV and -1.152 MeV respectively. As the Q-value of a reaction governs the probability of occurrence of a particular reaction channel, this difference in 1n stripping process from ${}^7\text{Li}+{}^{64}\text{Ni}$ to ${}^7\text{Li}+{}^{58}\text{Ni}$ can be reflected in the threshold behaviour of the interaction potential for the two isotopes.

2. Experimental Details

The experiments were carried out at 14UD BARC/TIFR Pelletron Facility in Mumbai, India. The self-supporting targets were prepared by electron gun evaporation technique from 99% enriched metallic ${}^{64}\text{Ni}$ isotope. A target of thickness $376 \mu\text{g}/\text{cm}^2$ was used for the two experiments. The targets were bombarded with ${}^6\text{Li}$ beam of energies 13, 14, 17, 19 and 26 MeV. For ${}^7\text{Li}$ the bombarding energies were 12, 14.3, 15, 16, 19.3 and 26.4 MeV. The beam current during the ${}^6\text{Li}+{}^{64}\text{Ni}$ experiment was varied from 1 to 7 pA and from 1 to 12 pA during the ${}^7\text{Li}+{}^{64}\text{Ni}$ experiment. The current was measured using a Current Integrator, the output of which was fed into a CAMAC Scaler to obtain the integrated charge. Conventional silicon surface barrier detector telescopes were used in the experiments to detect the elastically scattered particles. In the ${}^6\text{Li}$ experiment, the two telescopes were set with the ΔE detectors of thickness $15 \mu\text{m}$ and $10 \mu\text{m}$ followed by 3 mm and

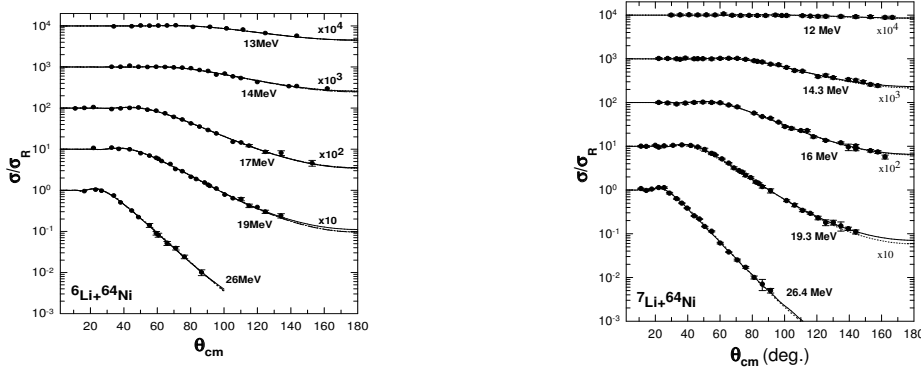


Figure 1: (Left) Elastic angular distributions of ${}^6\text{Li}+{}^{64}\text{Ni}$. The solid line represents prediction with the phenomenological potential. The dashed-dotted (dotted) curves are the predictions using the model potential OMP2 (OMP1). (Right) Elastic angular distributions of ${}^7\text{Li}+{}^{64}\text{Ni}$. The solid line represents prediction with the hybrid potential (OMP2). The dotted curves are the predictions using the phenomenological model potential.

500 μm E detectors. In the experiment involving the ${}^7\text{Li}$ projectile, four telescopes were set with 15 μm and 25 μm thick ΔE detectors and 500 μm and 3 mm thick E detectors to detect the heavy charged particles. The telescopes were placed on a rotatable arm at an angular separation of 20° for ${}^6\text{Li}$ and 10° for ${}^7\text{Li}$ experiment respectively. Two detectors of thickness 3 mm were mounted at $\pm 15^\circ$ about the beam axis at a distance of 40.7 cm to monitor the beam position and also for the purpose of normalization. The calibration runs were taken with a standard ${}^{209}\text{Bi}$ target after each energy change. The statistical error in the data is less than 1% in the forward angles and a maximum of 16% in the backwards angles. The overall error in the data varied from 5% to 17%. The data were recorded using the LINUX based data acquisition system LAMPS [2]. The average energy resolutions of the detectors were 286 keV for ${}^6\text{Li}+{}^{64}\text{Ni}$ experiment and 190-224 keV for ${}^7\text{Li}+{}^{64}\text{Ni}$ experiment approximately.

3. Analysis

The energy dependence of the surface strengths of the effective potential components are subsequently extracted in a model independent way by using three different model potentials—a phenomenological Woods-Saxon potential with *variable* geometry as energy changes, a *fixed* geometry folded DDM3Y potential with complex renormalization factor (OMP1) and a *hybrid* potential with *fixed* geometry real folded potential and *variable* geometry phenomenological imaginary potential (OMP2). The existing data for the systems ${}^{6,7}\text{Li}+{}^{58}\text{Ni}$ have, subsequently, been analyzed following the same prescriptions. The search code ECIS94 [3] was used to perform the model calculations. The measured elastic cross sections with respect to the Rutherford cross sections fitted with different model potentials for ${}^6\text{Li}+{}^{64}\text{Ni}$ and ${}^7\text{Li}+{}^{64}\text{Ni}$ have been shown in Fig. 1(Left) and (Right) respectively.

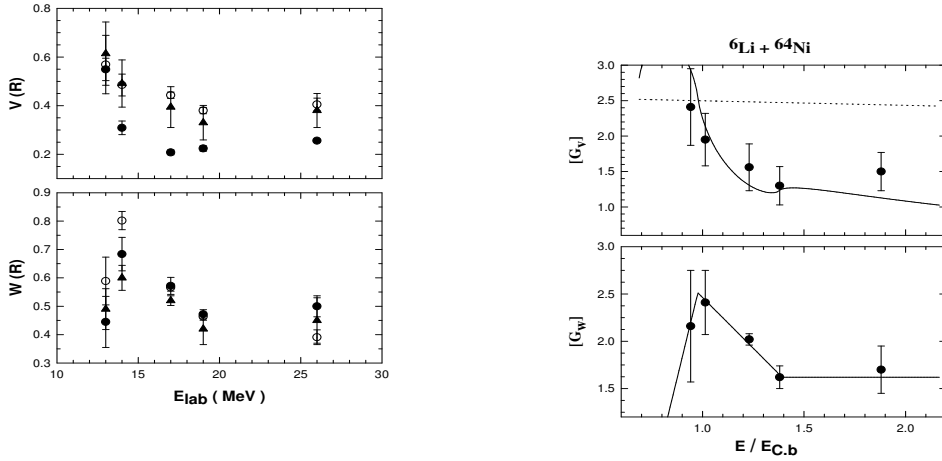


Figure 2: (Left) The real and imaginary surface strengths (at 9.8 fm) obtained with the phenomenological (solid circle), OMP1 (open circle) and OMP2 (solid triangle) model potentials for ${}^6\text{Li}+{}^{64}\text{Ni}$ system. (Right) Energy variations of Gauss weighted integral quantities of real and imaginary components of OMP2 for ${}^6\text{Li}+{}^{64}\text{Ni}$. The solid line in the upper panel is the dispersion relation prediction with 3-linear segment fit of the imaginary component. The dotted line in the upper panel depicts the intrinsic energy dependence of the Gauss weighted integral of unrenormalized real part of OMP2. $E_{C.b}=13.8$ MeV is the value of the Coulomb barrier for the said system in the laboratory [4]

4. Results

The real and imaginary components calculated of all the three model potentials used for the system ${}^6\text{Li}+{}^{64}\text{Ni}$, evaluated at 9.8 fm, have been compared in Fig. 2(Left). Except showing some difference in magnitude all the model potentials are depicting the similar threshold behaviour. To get the energy variation, the real and imaginary potentials have to be evaluated at a particular radius known as radius of sensitivity of optical model potential. Unlike the strongly bound system where this evaluation is done at strong absorption radius that has very weak energy dependence, the radius of sensitivity found by the technique of crossing radius for loosely bound nuclei depends strongly on energy [5]. Considering this energy variation of crossing radius, a Gauss-weighted radial moment of real and imaginary potentials around the average radius of sensitivity has been plotted as a function of energy for ${}^6\text{Li}+{}^{58,64}\text{Ni}$. By fitting the energy variation of the imaginary component with the help of a three linear segments, the dispersion integral has been evaluated and the predictions from the dispersion relation [6] (shown in Fig. 2(Right) for ${}^6\text{Li}+{}^{64}\text{Ni}$) corroborate with our experimental energy variation of real potential nicely [7]. So, finally, it can be concluded that though the evidence of breakup is distinct in the energy variation of the potential strengths for ${}^6\text{Li}+{}^{58,64}\text{Ni}$ systems, close to the barrier the variation is more in the line of conventional threshold anomaly.

From Fig. 3(Left), it can be inferred that the energy dependence of interaction potential for ${}^7\text{Li}+{}^{64}\text{Ni}$ shows normal threshold behaviour. The imaginary potential decreases as the bombarding energy approaches the barrier. The real potential shows the characteristic rise in the same energy domain though the rise is not very sharp in nature. On the other hand, for ${}^7\text{Li}+{}^{58}\text{Ni}$ (Fig. 3(Right)), the potential does not exhibit any significant energy dependence. On approaching the barrier both

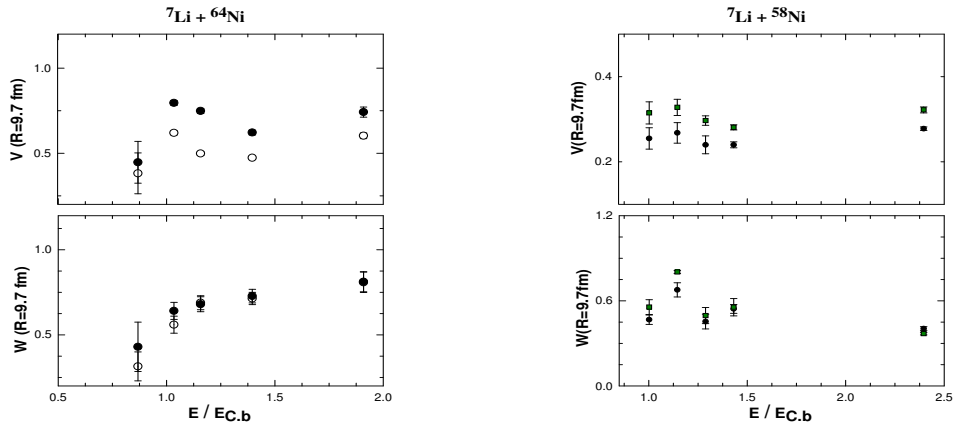


Figure 3: (Left) The real and imaginary surface strengths (at 9.7 fm) obtained with the phenomenological (open circle), OMP2 (solid circle) model potentials for ${}^7\text{Li}+{}^{64}\text{Ni}$ system, (Right) for ${}^7\text{Li}+{}^{58}\text{Ni}$, phenomenological (solid circle), OMP2 (solid square)

the real and imaginary potential strengths (except the 16 MeV data point) remain more or less flat. Thus the scattering of ${}^7\text{Li}$ from the Ni-isotopes studied suggests an isotopic dependence in the threshold behaviour of the effective potential for these systems.

Acknowledgements

The author would like to thank G. Ganguly from University of Calcutta for providing with the ${}^7\text{Li}$ -mass density values. The author also thanks the BARC/TIFR Pelletron staff for delivering the ${}^6,{}^7\text{Li}$ beams. Thanks are also due to Pradipta Das, B. P. Das from SINP for their help in preparing the targets and to Ajay K. Mitra from SINP for his extensive support during the experiment.

References

- [1] G. R. Satchler, Phys. Rep. 199 (1991) 147
- [2] LAMPS: Linux Advanced Multiparameter System; A. Chatterjee (private communication), <http://www.tifr.res.in/~pell/lamps.html>
- [3] J. Raynal, ECIS94, NEA 0850/16
- [4] R. A. Broglia and A. Winther, Heavy Ion Reactions, Vol. I: Elastic and Inelastic Reactions, Benjamin-Cummings Publishing Company, 1981
- [5] Mili Biswas, Phys. Rev. C 77 (2008) 017602
- [6] C. Mahaux, H. Ngo and G. R. Satchler, Nucl. Phys. A 449 (1986) 354 and Nucl. Phys. A 456 (1986) 134
- [7] M. Biswas *et al.*, Nucl. Phys. A 802 (2008) 67